

Trial of the cysteine cathepsin inhibitor JPM-OEt on early and advanced mammary cancer stages in the MMTV-PyMT-transgenic mouse model

Uta Schurig^{1,a}, Lisa Sevenich^{1,a}, Corinne Vannier¹, Mieczyslaw Gajda², Anne Schwinde¹, Fee Werner¹, Andreas Stahl³, Dominik von Elverfeldt⁴, Anne-Katrin Becker⁴, Matthew Bogoy⁵, Christoph Peters¹ and Thomas Reinheckel^{1,*}

¹Institut für Molekulare Medizin und Zellforschung, Albert-Ludwigs-Universität Freiburg, D-79104 Freiburg, Germany

²Institut für Pathologie, Friedrich-Schiller-Universität Jena, D-07740 Jena, Germany

³Universitäts-Augenklinik, Albert-Ludwigs-Universität Freiburg, D-79106 Freiburg, Germany

⁴Abteilung Röntgendiagnostik Medizin Physik, Albert-Ludwigs-Universität Freiburg, D-79106 Freiburg, Germany

⁵Department of Pathology, Stanford University School of Medicine, Stanford, CA 94305-5324, USA

*Corresponding author

e-mail: thomas.reinheckel@uniklinik-freiburg.de

Abstract

Recent data suggest proteases of the papain-like cysteine cathepsin family as molecular targets for cancer therapy. Here, we report the treatment of polyoma middle T oncogene-induced breast cancers in mice with the cell-permeable broad-spectrum cysteine cathepsin inhibitor JPM-OEt. Up to 100 mg/kg inhibitor was intraperitoneally injected once per day in two trials on early and advanced cancers. In both trials, transient delays in tumour growth were observed. However, at the endpoint of both experiments no significant differences in tumour weights, histopathology and lung metastasis were found between the inhibitor and the control group. The invasive strand formation of collagen I-embedded tumour cell spheroids generated from primary tumours of inhibitor-treated mice in the early cancer trial could be inhibited *in vitro* by JPM-OEt; a result arguing against induction of resistance to the inhibitor. Measurement of cysteine cathepsin activities in tissue extracts after intraperitoneal injection of JPM-OEt revealed effective inhibition of cysteine cathepsins in pancreas, kidneys and liver, while activities in mammary cancers and in lungs were not significantly affected. We conclude that the pharmacokinetic properties of JPM-OEt, which result in poor bioavailability, may prohibit its use for stand-alone treatment of solid mammary cancers and their lung metastases.

^aThese authors contributed equally to this work.

Keywords: pharmacokinetics; protease inhibitor; therapy.

Introduction

Proteases contribute to invasion and metastasis of solid cancers by degradation of extracellular matrix proteins and by shedding of bioactive peptides (Liotta and Kohn, 2001). Elevated expression and/or activity of certain endosomal/lysosomal cysteine proteases, i.e., cysteine cathepsins of the papain protease family, correlate with increased malignancy and poor prognosis of patients (Mohamed and Sloane, 2006). It has been experimentally established that tumour cells show enhanced secretion of endosomal/lysosomal cysteine proteases and these cathepsins have also been found to be associated to the extracellular side of the plasma membrane (Arkona and Wiederanders, 1996; Mai et al., 2000; Urbich et al., 2005; Lechner et al., 2006). Many lysosomal cysteine proteases are highly expressed by macrophages and other tumour-associated immune cells, which are thought to release cathepsins into the environment of the developing cancer or metastases (Gocheva et al., 2006; Vasiljeva et al., 2006). Acidification of the tumour microenvironment by tumour hypoxia and the release of the content of acidic vesicles are thought to establish favourable conditions for extracellular proteolytic activity of cathepsins (Gocheva and Joyce, 2007). In addition, intracellular cathepsins are known to regulate proliferation by modulating growth factor signalling and transcription factor processing and to interfere with several cell death pathways (Authier et al., 1999; Reinheckel et al., 2005; Goulet et al., 2007; Vasiljeva and Turk, 2008). Based on these data, inhibition of cysteine cathepsin activity has been envisaged as a potential therapeutic strategy against cancer. Mouse models of human cancer in which a *de novo* carcinogenic process is induced by cell type-specific expression of oncogenes provide attractive systems to test the *in vivo* efficacy of cysteine cathepsin inhibitors in cancer treatment (Frese and Tuveson, 2007). The irreversible inhibitor of papain-like cysteine cathepsins JPM-565/JPM-OEt is a derivative of the well established epoxysuccinyl-type compound E64 (Meara and Rich, 1996). The ester form JPM-OEt is cell permeable, while the acid JPM-565 is not. In a seminal study on the Rip1-Tag2 model of pancreatic islet cancer, Joyce and co-workers established that the intraperitoneal (i.p.) injection of JPM-OEt could prevent progression of carcinogenic precursor lesions and even reduce the size of already established cancers (Joyce et al., 2004). However, the Rip1-Tag2 pancreatic tumours are highly angiogenic nodules that do not establish distant metastases. Hence, we sought to test this

inhibitor in the highly invasive and metastatic MMTV-PyMT-transgenic mouse model of human breast cancer (Guy et al., 1992). In this model, the polyoma virus middle T oncogene (PyMT) is under the control of the mouse mammary tumour virus (MMTV) long terminal repeat promoter that directs expression of the oncogene to the epithelia of mammary ducts. Specifically, we aimed to apply the inhibitor to small macroscopically undetectable lesions and to use it for treatment of cancers with considerable sizes around the time of metastasis initiation, which mimics a clinically relevant setting.

Results

The MMTV-PyMT-transgenic mouse model of human breast cancer is characterised by a defined time course of primary tumour development and lung metastases formation in female mice (Figure 1A). First tumours and lung metastases can be detected at approximately 25 and 63 days of age, respectively. At 14 weeks (98 days of age) the primary tumours reach a final size exceeding 1 cm in diameter, and 100% of female mice develop lung metastases. Two treatment protocols have been employed to test the effect of the broad spectrum cysteine cathepsin inhibitor JPM-OEt on tumour progression: (i) a trial inter-

fering with advanced metastatic breast cancer in which treatment was started at 63 days of age, and (ii) a trial aiming at early stages of MMTV-PyMT-induced carcinogenesis starting on day 28 (Figure 1A). For testing whether the solvent of the inhibitor [70% phosphate buffered saline (PBS)/30% dimethylsulfoxide (DMSO)] shows toxic effects after i.p. injection, mice were injected once per day with PBS (n=3) or 30% DMSO/70% PBS (n=3) in a total volume of 125 μ l for 3 days or left untreated (n=3). We compared the histomorphology and the number of apoptotic/necrotic cells [by terminal dUTP nick-end labelling (TUNEL) staining] of lungs, kidney, liver and pancreas 2 h after the last injection. The number of TUNEL-positive cells was very low and not different in all groups (data provided for review). Likewise, there was no indication for toxicity of DMSO in the haematoxylin and eosin (HE)-stained histological sections of the tissues.

Validation of palpation score by magnetic resonance imaging

Because we determined tumour growth in MMTV-PyMT-transgenic mice by palpation using a semi-quantitative score, we validated the palpation approach by measuring tumour volumes using magnetic resonance imaging (MRI; Figure 1B). We found a significant correlation between the palpation score and the tumour volumes of female MMTV-PyMT-transgenic mice that were analysed weekly from week 5 to week 14 of age (Figure 1C). Therefore, the validated palpation score was used further in this study.

Trial on advanced MMTV-PyMT-induced mammary cancer

First, we investigated the influence of broad spectrum cysteine cathepsin inhibitor JPM-OEt in an intervention setting on already established tumours and early metastases by daily i.p. injection of JPM-OEt (50 mg/kg) from day 63 to day 98 in MMTV-PyMT-transgenic mice, while tumour bearing mice of the control group were injected with the inhibitor solvent (70% PBS/30% DMSO). Tumour sizes of mice from the control and inhibitor groups were matched at the beginning of inhibitor treatment. JPM-OEt injection caused a significant delay in the increase of tumour burden during the first 2 weeks of treatment (Figure 2A). However, on days 84, 91 and 98 no significant differences between both groups could be detected (Figure 2A). Determination of the tumour weights on day 98 with no significant difference between the inhibitor and control groups confirmed the palpation results (Figure 2B). Further, histopathological grading of HE-stained paraffin sections of right thoracic tumours did not reveal any significant differences between the control and inhibitor groups (Figure 2C).

The metastatic burden in lungs at the end of treatment did not reveal any significant differences between the control and inhibitor groups, as shown by real-time PCR for PyMT expression and histology (Figure 3A,B). The fraction of tumour cells in lung metastases expressing the proliferation marker protein Ki67 was not significantly different in the inhibitor group compared to the control group (Figure 3C,D). In addition, there were no differenc-

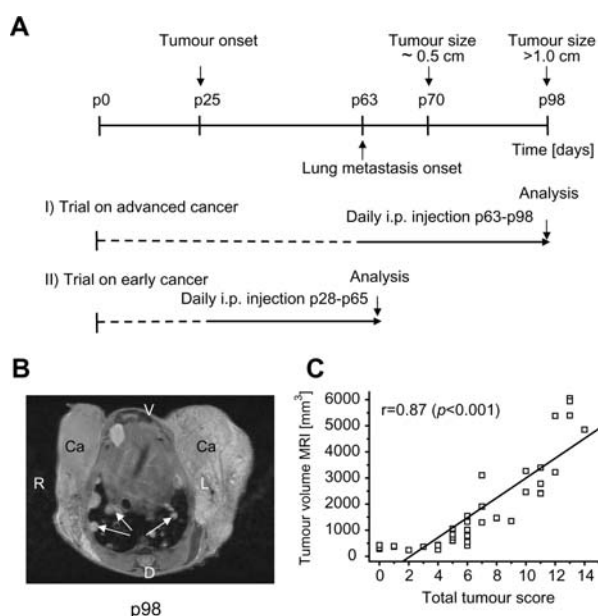


Figure 1 Time course of JPM-OEt trials and correlation of palpation score with tumour volume determined by magnetic resonance imaging (MRI).

(A) The upper scheme shows the normal time course of breast cancer development and lung metastasis in female MMTV-PyMT-transgenic mice. The two schemes below depict the JPM-OEt treatment regimen in the trials on early (I) and advanced cancers (II). (B) Representative MRI image of advanced MMTV-PyMT-induced cancer. V=ventral, D=dorsal, R=right, L=Left, Ca=breast cancer; the white arrows point to lung metastases. (C) Tumour volumes of the upper six mammary glands of five MMTV-PyMT-transgenic mice were determined by palpation using the semi-quantitative score followed by quantification of successive MRI sections. The measurements were started at an age of 5 weeks and continued once per week until an age of 14 weeks; the graph presents the correlation between palpation score and MRI measured tumour volume.

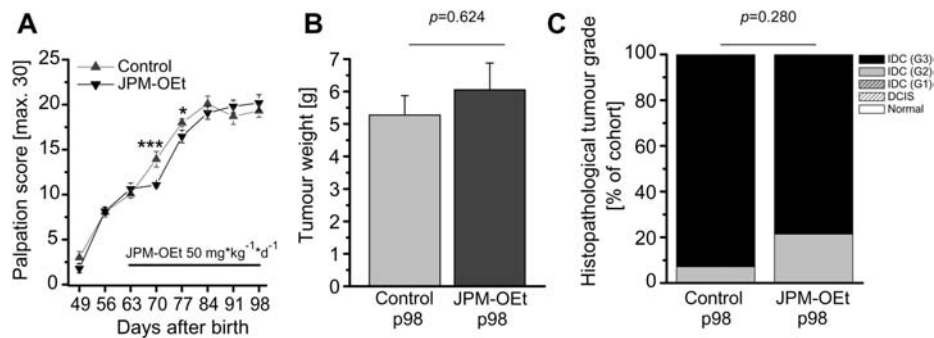


Figure 2 Advanced cancer trial: progression of primary tumours.

Intraperitoneal injection of JPM-OEt in the inhibitor group ($n=14$) and solvent in the control group ($n=12$) was performed daily during the time span from 63 to 98 days of age. (A) Tumour volumes were estimated by palpation using a semi-quantitative score. (B) Total tumour weight of all 10 mammary glands at study end (day 98). (C) Histopathology of the upper left thoracic mammary gland. Normal=normal gland structure; DCIS=ductal carcinoma *in situ*; IDC=invasive ductal carcinoma; well differentiated grade I (G1), moderately differentiated grade II (G2), or poorly differentiated grade III (G3). Data are presented as means \pm SEM or as percentage proportions of the cohort. * $p<0.05$, *** $p<0.001$.

es in the number of TUNEL-positive apoptotic/necrotic cells in the metastases of the two mouse cohorts (Figure 3E,F). Together, these data indicate that formation and

growth rate of lung metastases was not affected by JPM-OEt treatment.

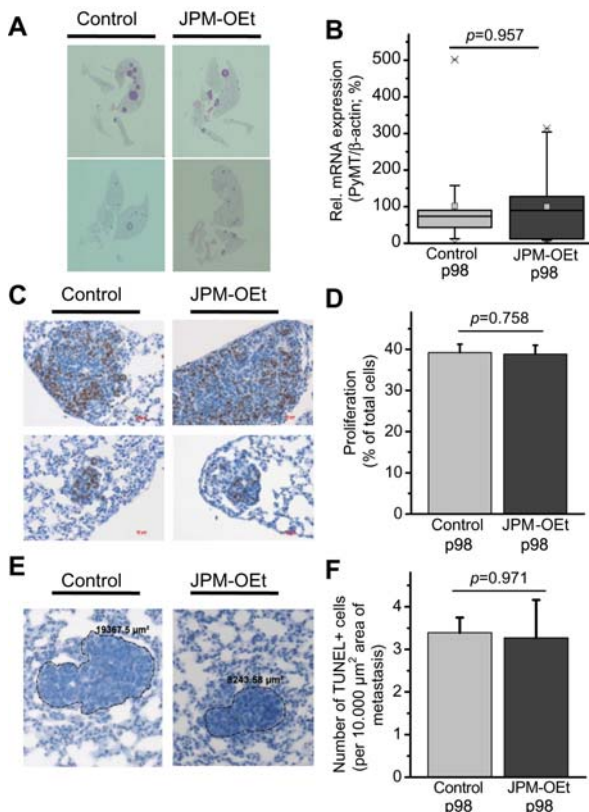


Figure 3 Advanced cancer trial: lung metastasis formation and proliferation of tumour cells in lung metastases.

(A) Representative sections of right lung lobes with metastases in 98-day-old MMTV-PyMT-transgenic mice. (B) Lung metastasis burden in the left lung lobes by RTQ-PCR quantification of PyMT mRNA expression. (C) Representative Ki67-stained histological sections of metastases of right lung lobes. (D) Quantification of tumour cell proliferation in lung metastases by Ki67 immunohistochemistry (control group: $n=12$, JPM-OEt group: $n=14$). (E) Representative TUNEL-stained histological sections of metastases in right lung lobes. The areas (in μm^2) of the encircled metastases are presented. (F) Quantification of apoptotic/necrotic cells in lung metastases by TUNEL staining (control group: $n=4$, JPM-OEt group: $n=5$).

Trial on early MMTV-PyMT-induced mammary cancer

To test whether JPM-OEt affects the early development of MMTV-PyMT breast cancer, we initiated an inhibitor trial starting at 28 days of age. At this time point, tumours are not palpable. However, detailed histological examination of mammary tissue revealed a considerable frequency of small invasive ductal carcinomas already at this stage (Figure 4A). After initiation of treatment by daily i.p. injection of 100 mg/kg JPM-OEt or solvent, the tumours progressed to a similar extent in the inhibitor and control groups until the endpoint of the study at 65 days of age (Figure 4). Only at a single time point at 47 days of age did the inhibitor-treated mice show a significant reduction in tumour size; however, the extent of this effect is minor (Figure 4B). At the end of the treatment, there were no differences in tumour size and tumour weight in both groups (Figure 4B,C). In the control group, two out of 13 mice had developed histologically evident lung metastases, while one metastasis was found in the inhibitor-treated mice. However, this finding was not significant (data not shown).

Tumour cells of JPM-OEt-treated mice are sensitive to the inhibitor

After long-term application of drugs, the development of drug resistance is a common problem in cancer therapy that could potentially explain the overall failure of JPM-OEt in reducing progression of MMTV-PyMT-induced cancers. To address this hypothesis, we isolated primary cancer cells from JPM-OEt- and solvent-treated MMTV-PyMT-transgenic mice after 37 days of treatment at the end of the trial on early cancers. The primary cells were used to generate three-dimensional tumour cell spheroids that were subsequently embedded in a collagen I matrix (Figure 5A). The collagen-embedded spheroids were exposed *in vitro* to JPM-OEt at a final concentration of 80 μM . Control assays were performed with the solvent of inhibitor. The sprouting of tumour cell spheroids

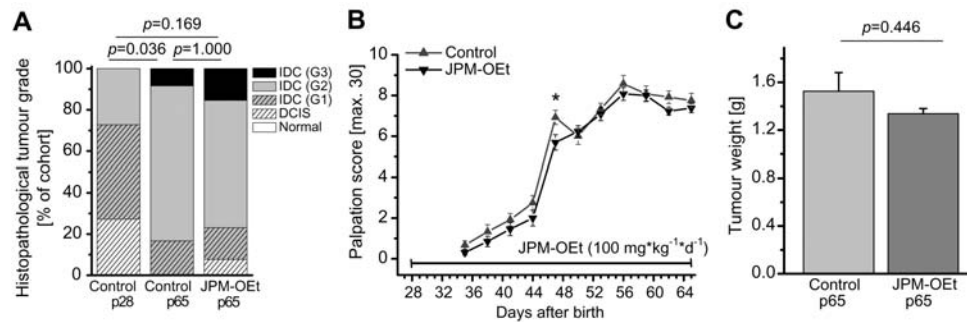


Figure 4 Early cancer trial: progression of primary tumours.

Intraperitoneal injection of JPM-OEt in the therapy group ($n=13$) and solvent in the control group ($n=12$) was performed daily during the time span from 28 to 65 days of age. (A) Histopathology of the upper left thoracic mammary gland. Normal=normal gland structure; DCIS=ductal carcinoma *in situ*; IDC=invasive ductal carcinoma; well differentiated grade I (G1), moderately differentiated grade II (G2), or poorly differentiated grade III (G3). (B) Tumour volumes were estimated by palpation using a semi-quantitative score $p<0.05$. (C) Comparison of total tumour weight of all 10 mammary glands at day p65. Data are presented as means \pm SEM or as percentage proportions of the cohort.

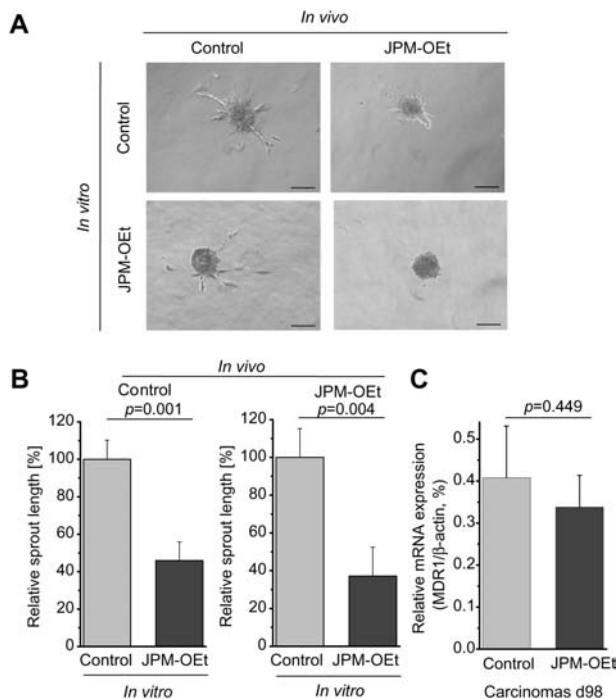


Figure 5 Inhibition of tumour cell spheroid sprouting by JPM-OEt.

Collagen I-embedded tumour cell spheroids of primary tumour cells from MMTV-PyMT-transgenic mice from either the inhibitor or control groups of the early cancer study. (A) Representative tumour cell spheroids from MMTV-PyMT-transgenic mice of the control and JPM-OEt groups (*in vivo*) either untreated (control) or treated with JPM-OEt *in vitro*. (B) Relative sprout length of tumour cells embedded in a collagen I matrix. Data are presented as means \pm SEM. (C) RTQ-PCR for the multidrug resistance protein *Mdr1* determined in control and inhibitor-treated primary breast cancers from 98-day-old mice ($n=3$). Data are presented as means \pm SEM.

in the collagen matrix was quantified as measure of invasiveness. We found that invasive strand formation of tumour cells from both the inhibitor and control groups of the *in vivo* study was significantly reduced after application of JPM-OEt *in vitro* (Figure 5B). In addition, mRNA expression of the multidrug resistance protein 1 [*Mdr1*, alternative nomenclature: ABC-transporter B1; P-glyco-

protein (Gottesman et al., 2002)] in day 98 primary tumours was measured by quantitative real-time PCR (RTQ-PCR) (Figure 5C). There was no significant difference in *Mdr1* expression between the control and inhibitor groups. Hence, *in vivo* JPM-OEt treatment did not result in resistance to the inhibitor and is unlikely to induce multidrug resistance.

Expression and activity of cysteine cathepsins in organs and tumours of JPM-OEt-treated mice

Treatment of the Rip1-Tag2 model of pancreatic islet cancer with JPM-OEt resulted in impaired angiogenic switching in progenitor lesions, as well as reduced tumour growth, vascularity and invasiveness (Joyce et al., 2004). However, our present study could detect only transient or minor effects after daily injection of JPM-OEt in the MMTV-PyMT-transgenic breast cancer model. Thus, we tested the *in vivo* efficacy on cysteine cathepsin inhibition of i.p.-injected JPM-OEt in various tissues, including mammary cancers. First, we injected control solvent or JPM-OEt into wild-type animals (100 mg/kg/d) for 3 days and prepared tissue extracts 2 h after final injection. Degradation of the fluorogenic peptide Z-Phe-Arg-AMC, which is mainly cleaved by cathepsins B and L, was measured in pancreas, kidneys, liver and lungs (Figure 6A). Strikingly, the degradation of the fluorogenic substrate was nearly abolished in the organs close to the injection site, i.e., the peritoneal cavity. In contrast, the lungs showed only a moderate non-significant reduction of substrate cleavage. We further measured Z-Phe-Arg-AMC degradation in primary tumour extracts at the end of the early and advanced cancer inhibitor trials on day 65 and day 98, respectively (Figure 6B,C). However, in both settings only non-significant reductions of cathepsin B/L activity were found. To investigate possible effects of JPM-OEt treatment on cathepsin expression at mRNA level, we measured cathepsins B, L and X/Z by RTQ-PCR in day 98 primary tumours (Figure 6D). However, expression levels were not affected after inhibitor application. Hence, it appears that JPM-OEt treatment might not efficiently inactivate its target proteases in primary MMTV-

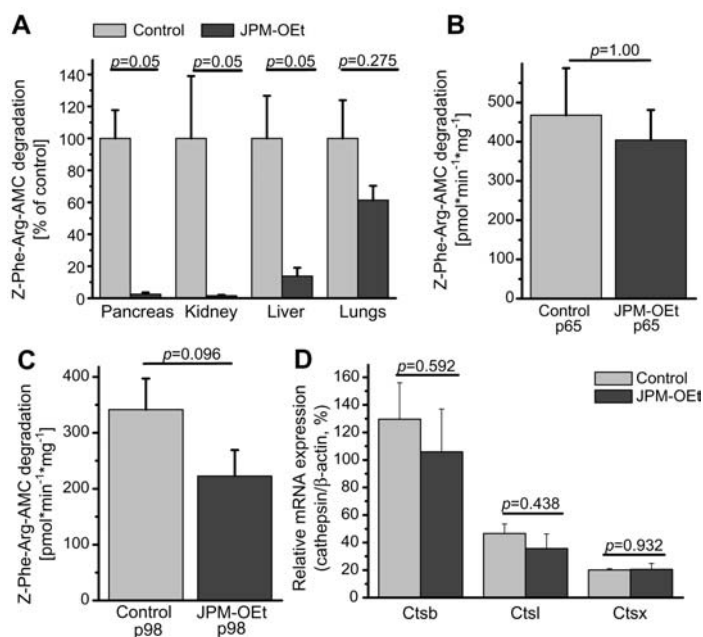


Figure 6 Efficacy of cysteine protease inhibition after intraperitoneal injection of JPM-OEt.

(A) JPM-OEt (100 mg/kg) was injected daily into wild-type mice for 3 days ($n=3$). Control mice were treated with the solvent DMSO/PBS ($n=3$). Liver, lungs, kidneys and pancreas were prepared 2 h after the final injection and cysteine cathepsin activity was measured by degradation of the fluorogenic peptide Z-Phe-Arg-AMC. (B) Z-Phe-Arg-AMC degradation in tissue homogenates of left cervical mammary cancers prepared 2 h after the final injection of the early cancer and (C) advanced cancer trials. (D) Comparison of mRNA expression of cathepsin B (*Ctsb*), cathepsin L (*Ctsl*) and cathepsin X (*Ctsx*) in tumour samples from the advanced cancer trial by RTQ-PCR. Data are presented as means \pm SEM.

PyMT-induced breast cancers and in the lungs as target tissue of breast cancer metastasis in this tumour model.

Discussion

Crossing mouse lines with single deficiencies for various cysteine cathepsins to the transgenic mouse models for Rip1-Tag2-induced pancreatic islet cell cancer and MMTV-PyMT-induced breast cancer provided clear evidence for critical involvement of cathepsins L, B and S in distinct tumorigenic processes (for a review, see Vasiljeva et al., 2007). On the other hand, cathepsin L deficiency has been shown to result in a number of spontaneous phenotypes, such as cardiomyopathy, reduction of CD4-positive T-helper lymphocytes, periodic hair loss and epidermal hyperplasia (Nakagawa et al., 1998; Reinheckel et al., 2005; Petermann et al., 2006; Spira et al., 2007). There is also clear evidence for functional compensation amongst members of the cysteine cathepsin family. Most notably, combined deficiency for cathepsins B and L causes a severe hypotrophic and neurodegenerative phenotype and death of the mice within a few weeks after birth (Felbor et al., 2002; Sevenich et al., 2006). Hence, complete inhibition of cysteine cathepsin activities by gene targeting results in anti-tumour effects as well as in some spontaneous disease phenotypes that can be interpreted as 'toxic' effects of long-term cathepsin inactivation. In contrast, *in vivo* testing of cysteine cathepsin inhibitors based on epoxysuccinyl reactive groups, such as natural product E64 and its derivative JPM-565/JPM-OEt, revealed virtually no toxicity of these compounds even at doses up to 100 mg/kg (Sadaghiani

et al., 2007). One likely reason for the well tolerated application of the inhibitor is its pharmacokinetic characteristics. Intraperitoneal injection of 50 mg/kg JPM-OEt results in high plasma concentrations of approximately 50 μM 15–20 min after injection. However, during the next 30 min the plasma concentration of the inhibitor drops to less than 10 μM (Sadaghiani et al., 2007). It is of great interest that in this pharmacokinetic study only the JPM-565, which lacks cell permeability, was detected in the plasma. This is due to the rapid conversion of the injected cell permeable ethyl ester JPM-OEt to its corresponding acid JPM-565 in the serum. This is in line with our measured cysteine cathepsin activities in various tissue extracts and tumours. A substantial reduction of cathepsin activity after i.p. injection of JPM-OEt was only detected in organs with direct contact to the peritoneum, i.e., pancreas, kidneys and liver. Hence, it is likely that JPM-OEt could access these tissues in its cell permeable form without significant exposure to serum esterases. In contrast, tissues that can be reached by the inhibitor only via circulation, i.e., lungs and mammary tumours, showed comparably small and non-significant reductions in active cysteine cathepsins. The small inhibitory effects observed in lungs and tumours might result from inhibition of extracellular occurring cysteine cathepsins. However, the 'negative' results of our present trials on early and advanced mammary cancer stages in the MMTV-PyMT-transgenic mouse model indicate that downregulating a small, eventually extracellular, proportion of cathepsin activity is not sufficient to cause a substantial inhibition of mammary cancer progression and lung metastasis in this model. In this regard, it is noteworthy that Rip1-Tag2-induced pancreatic islet cell cancer was

successfully treated with daily i.p. injection of 50 mg/kg JPM-OEt (Joyce et al., 2004), a dose that is, according to our present data and the recent data of Sadaghiani et al. (2007), sufficient to cause substantial cysteine cathepsin inhibition in the pancreas. Consequently, JPM-OEt appears to be a substance that could be tested in further tumour models with good accessibility for the drug. One important condition to target could be the peritoneal carcinosis associated with ovarian cancer, a tumour entity for which increased expression of cathepsin B has been shown (Downs et al., 2005). In contrast, improved pharmacokinetics and cell permeability of cathepsin inhibitors appear to be a necessity to use these compounds for systemic treatment of large solid cancers, such as the mammary cancers of the MMTV-PyMT-transgenic mouse. However, according to the lessons learned from the cathepsin knockout mice, long-term systemic ablation of cysteine cathepsins might result in substantial toxicity. Thus, use of stable and cell-permeable selective inhibitors that target individual tumour promoting cathepsins that do not show gross phenotypes in the knockout model, e.g., cathepsin B, might represent a therapeutic advantage. Another recent approach employed JPM-OEt in combination with conventional chemotherapy regimen and showed additive anti-tumour effects in the Rip1-Tag2 model (Bell-McGuinn et al., 2007). Although the molecular mechanisms of this additive effect are unknown to date, it offers the chance to use the essentially non-toxic JPM-OEt to enhance the therapeutic efficacy of standard chemotherapy of cancer.

In conclusion, our present data indicate that substantial cysteine cathepsin inhibition is required to achieve a decent anti-tumour effect and therefore the pharmacokinetic properties of JPM-OEt may prevent the use of this compound as a stand-alone option for cancer treatment. However, improved small molecule cathepsin inhibitors in combination with novel chemotherapeutic treatment strategies, which can be tested in mouse models, such as the MMTV-PyMT-transgenic breast cancer model, have the potential to become valuable therapeutics of metastatic malignant disease.

Materials and methods

Animals

Female mice of a transgenic mouse strain expressing the PyMT oncogene under the control of MMTV LTR promoter [FVB/N-TgN(MMTVPyVT)634Mul/J (Guy et al., 1992)], here designated as MMTV-PyMT-transgenic mice, were used for therapeutic studies. Animals were kept under standard conditions, fed with a standard diet and given free access to water. All animal studies were approved by the government commission for animal protection of the Regierungspräsidium Freiburg (AZ 35-9185.81/3 G-06/17).

Therapeutic studies

The cysteine cathepsin inhibitor JPM-OEt was dissolved in 70% PBS/30% DMSO and administered daily by i.p. injection. Control groups were treated with 70% PBS/30% DMSO. For the advanced cancer trial, the daily JPM-OEt dose was 50 mg/kg injected from day 63 to day 98 after birth. Treatment-blinded

estimation of tumour size was performed by palpation once per week. In the trial on early cancers, 100 mg/kg JPM-OEt was injected daily from day 28 to day 65 after birth; palpation was performed every 3rd day. Analyses of mice from both trials were performed on the day of the final injection.

Palpation score

Tumour size of MMTV-PyMT-transgenic mice was estimated using a semi-quantitative palpation score (0 points: tumour not palpable, 1 point: <0.5 cm, 2 points: 0.5–1.0 cm, 3 points: >1.0 cm), with a maximal palpation score of 30 points per animal (10 mammary glands per mouse).

Magnetic resonance imaging

For MRI measurements, a 94/20 Bruker BioSpec System with a BGA 12S (Bruker BioSpin, Ettlingen, Germany) was employed. Furthermore, a mouse whole body quadrature birdcage coil, with an inner diameter of 36 mm, was used. The imaging protocol consisted of a total of three sequences in six scans. After two pilot sequences of which the respiration triggered, second, multi-slice one was used for slice orientation planning, a FLASH based T_1 -weighted and a T_2 -weighted RARE sequence were run. The FLASH sequence had an Echo Time Repetition Time (TE/TR) of 5.4/980 ms, a bandwidth of 50 kHz and a flip angle of 40°. The RARE sequence had a TE/TR of 42/10°800 ms, a turbo-factor of 8 and a bandwidth of 35 kHz. The T_1 and T_2 sequences were both run twice, with slice packages of 30 axial slices covering the upper torso ranging from caudal of the calvarium until the cranial end of the iliac crest. Slice thickness was 600 μm with an in-plane resolution of 117×117 μm and a matrix of 256×256 resulting in a field of view of 3×3 cm. Determination of tumour volumes was performed via manual segmentation. Via a Matlab® based custom built tool for region definition, and guided by the two different image contrasts, each tumour was circumscribed in each image slice. Total left and right tumour volumes were calculated multiplying the number of segmented image pixels with the corresponding pixel volume.

Histological analyses

Tumour tissue of left thoracic mammary glands and complete lung lobes were fixed in 4% phosphate-buffered paraformaldehyde, subsequently dehydrated and embedded in paraffin wax. Frontal tumour sections (5 μm) were applied for histopathological assessment and stained with HE, according to standard procedures. Tumours of MMTV-PyMT-transgenic mice were graded in a blinded setting by a pathologist into defined stages: normal gland (N), atypical ductal hyperplasia (ADH), ductal carcinoma *in situ* (DCIS) and invasive ductal carcinoma (IDC). The latter stage was further characterised by a three-grade system (GI, GII, GIII) with respect to nuclear hyperchromasia, mitotic activity, tubule and cellular differentiation (Elston and Ellis, 1991). Lung sections (5 μm) were applied for immunohistochemical staining using anti-Ki67 antibody (Dako A/S, Glostrup, Denmark; 1:10 dilution). Peroxidase-based detection of the primary antibodies was performed according to the instructions of the Vectastain-Elite-ABC-Kit (Vector Laboratories Inc., Burlingame, USA). DNA fragmentation of apoptotic/necrotic cells was detected by *in situ* labelling DNA strand breaks by the TUNEL procedure (ApopTag; Oncor, Temecula, USA). Five metastases in lung sections of each animal were photographed using a 40× objective lens. Ki67 proliferation index was calculated as the number of Ki67-positive tumour cell nuclei expressed as a percentage of the total cell number. Apoptotic/necrotic cells were counted and normalised to the area of metastasis determined by the Axio Vision LE 4.4 software (Carl Zeiss, Oberkochen, Germany).

Quantitative real-time PCR

An entire lung lobe was used to determine the relative expression of PyMT transgene to determine the metastatic burden in lungs. Total RNA was isolated from lungs and mRNA was reversely transcribed into cDNA. RTQ-PCR was performed by detection of SYBR-green dye DNA-intercalation in newly formed PCR-products using the MyiQ™ single-colour real-time PCR detection system (Bio-Rad, Hercules, USA). The relative amount of target gene expression was normalised to the β -actin transcripts.

Primers: PyMT.1: 5'-CTC CAA CAG ATA CAC CCG CAC ATA CT-3'; PyMT.2: 5'-GCT GGT CTT GGT CGC TTT CTG GAT AC-3'; *Ctsb*.1: 5'-CCT GGG CTG GGG AGT AGA GAA TGG AG-3'; *Ctsb*.2: 5'-TGG AAA AAG CCC CTA AGG ACT GGA CAA T-3'; *Ctsl*.1: 5'-GCA CGG CTT TTC CAT GGA-3'; *Ctsl*.2: 5'-CCA CCT GCC TGA ATT CCT CA-3'; *Ctsx*.1: 5'-TAT GCC AGC GTC ACC AGG AAC-3'; *Ctsx*.2: 5'-CCT CTT GAT GTT GAT TCG GTC TGC-3'; *Mdr1.1*: 5'-TCG AAG ATG GGC AAA AAG AGT AAA-3'; *Mdr1.2*: 5'-CCA TGG ATA ATA GCA GCG AGA GT-3'; β -*actin*.1: 5'-ACC CAG GCA TTG CTG ACA GG-3'; β -*actin*.2: 5'-GGA CAG TGA GGC CAG GAT GG-3'.

Generation of sprouting spheroids from primary MMTV-PyMT tumour cells

Primary tumour cells from animals of the inhibitor and control group were obtained by mechanical and enzymatic dissociation of solid MMTV-PyMT-induced carcinomas, as previously described (Gocheva et al., 2006; Vasiljeva et al., 2006). The obtained suspension was sequentially transferred through 100 and 40 μ m cell strainers, washed twice with PBS, and cultured for 24 h at 37°C and 5% CO₂. Vital and adherent cells were harvested by trypsin incubation, followed by PBS wash and subsequent suspension in cell culture medium (Dulbecco's modified Eagle's medium, 10% fetal calf serum, 1% L-glutamine, 1% penicillin/streptomycin) with addition of 0.24% (w/v) methylcellulose. Droplets (25 μ l), each containing approximately 1000 primary tumour cells, were applied to a plastic cell culture plate that was subsequently flipped around. All suspended cells contributed to the formation of a single three-dimensional spheroid in a 'hanging droplet' during an incubation time of 24 h. Spheroids were finally harvested, seeded in a collagen type I matrix (2 mg/ml) and exposed to JPM-OEt at a final concentration of 80 μ M *in vitro*. The length of sprouts was measured after 24 h using the Axio Vision LE 4.4 software (Carl Zeiss, Oberkochen, Germany).

Cathepsin activity assay

Frozen tissues of primary tumours, lungs, kidneys, pancreas and liver (250 mg) were disrupted in 500 μ l NaAc buffer (200 mM sodium acetate, 1 mM EDTA, 0.05% Brij 35, pH 5.5) using an Ultrathurrax (IKA, Staufen, Germany) followed by Dounce homogenisation (Wheaton Millville, USA) and centrifugation at 1000 g for 15 min. Proteolytic activity was determined by degradation of the fluoropeptide Z-Phe-Arg-4-methyl-coumarin-7-amide (Z-Phe-Arg-AMC, 25 μ M; Bachem, Bubendorf, Switzerland) in NaAc buffer with prior addition of 0.5 mM dithiothreitol. The release of 7-amino-4-methyl-coumarin was continuously monitored for 45 min by spectrofluorometry at excitation and emission wavelengths of 360 nm and 460 nm, respectively.

Statistics

Statistical analyses were performed with the Xlstat™ add-on to the Microsoft Excel 2003™ software (Addinsoft, Paris, France). Comparison of tumour grade frequencies was carried out with χ^2 -test. Owing to large differences in the variances between groups, the palpation data were analysed by the non-parametric

Mann-Whitney U-test. For each test, $p \leq 0.05$ was considered to be statistically significant.

Acknowledgements

This study was supported by the European Union Framework Programme 6, Project LSHC-CT-2003-503297 (Cancer-Degradome) and by the state of Baden-Württemberg, Germany: AZ 23-7532.22-35-11/2.

References

- Arkona, C. and Wiederanders, B. (1996). Expression, subcellular distribution and plasma membrane binding of cathepsin B and gelatinases in bone metastatic tissue. *Biol. Chem.* 377, 695–702.
- Autherier, F., Metioui, M., Bell, A.W., and Mort, J.S. (1999). Negative regulation of epidermal growth factor signaling by selective proteolytic mechanisms in the endosome mediated by cathepsin B. *J. Biol. Chem.* 274, 33723–33731.
- Bell-McGuinn, K.M., Garfall, A.L., Bogyo, M., Hanahan, D., and Joyce, J.A. (2007). Inhibition of cysteine cathepsin protease activity enhances chemotherapy regimens by decreasing tumor growth and invasiveness in a mouse model of multistage cancer. *Cancer Res.* 67, 7378–7385.
- Downs, L.S. Jr, Lima, P.H., Bliss, R.L., and Blomquist, C.H. (2005). Cathepsins B and D activity and activity ratios in normal ovaries, benign ovarian neoplasms, and epithelial ovarian cancer. *J. Soc. Gynecol. Invest.* 12, 539–544.
- Elston, C.W. and Ellis, I.O. (1991). Pathological prognostic factors in breast cancer. I. The value of histological grade in breast cancer: experience from a large study with long-term follow-up. *Histopathology* 19, 403–410.
- Felbor, U., Kessler, B., Mothes, W., Goebel, H.H., Ploegh, H.L., Bronson, R.T., and Olsen, B.R. (2002). Neuronal loss and brain atrophy in mice lacking cathepsins B and L. *Proc. Natl. Acad. Sci. USA* 99, 7883–7888.
- Frese, K.K. and Tuveson, D.A. (2007). Maximizing mouse cancer models. *Nat. Rev. Cancer* 7, 645–658.
- Gocheva, V. and Joyce, J.A. (2007). Cysteine cathepsins and the cutting edge of cancer invasion. *Cell Cycle* 6, 60–64.
- Gocheva, V., Zeng, W., Ke, D., Klimstra, D., Reinheckel, T., Peters, C., Hanahan, D., and Joyce, J.A. (2006). Distinct roles for cysteine cathepsin genes in multistage tumorigenesis. *Genes Dev.* 20, 543–556.
- Gottesman, M.M., Fojo, T., and Bates, S.E. (2002). Multidrug resistance in cancer: role of ATP-dependent transporters. *Nat. Rev. Cancer* 2, 48–58.
- Goulet, B., Sansregret, L., Leduy, L., Bogyo, M., Weber, E., Chauhan, S.S., and Nepveu, A. (2007). Increased expression and activity of nuclear cathepsin L in cancer cells suggests a novel mechanism of cell transformation. *Mol. Cancer Res.* 5, 899–907.
- Guy, C.T., Cardiff, R.D., and Muller, W.J. (1992). Induction of mammary tumors by expression of polyomavirus middle T oncogene: a transgenic mouse model for metastatic disease. *Mol. Cell. Biol.* 12, 954–961.
- Joyce, J.A., Baruch, A., Chehade, K., Meyer-Morse, N., Giraudo, E., Tsai, F.Y., Greenbaum, D.C., Hager, J.H., Bogyo, M., and Hanahan, D. (2004). Cathepsin cysteine proteases are effectors of invasive growth and angiogenesis during multistage tumorigenesis. *Cancer Cell* 5, 443–453.
- Lechner, A.M., Assfalg-Machleidt, I., Zahler, S., Stoekelhuber, M., Machleidt, W., Jochum, M., and Nagler, D.K. (2006). RGD-dependent binding of procathepsin X to integrin $\alpha 3$ mediates cell-adhesive properties. *J. Biol. Chem.* 281, 39588–39597.

- Liotta, L.A. and Kohn, E.C. (2001). The microenvironment of the tumour-host interface. *Nature* **411**, 375–379.
- Mai, J., Finley, R.L. Jr, Waisman, D.M., and Sloane, B.F. (2000). Human procathepsin B interacts with the annexin II tetramer on the surface of tumor cells. *J. Biol. Chem.* **275**, 12806–12812.
- Meara, J.P. and Rich, D.H. (1996). Mechanistic studies on the inactivation of papain by epoxysuccinyl inhibitors. *J. Med. Chem.* **39**, 3357–3366.
- Mohamed, M.M. and Sloane, B.F. (2006). Cysteine cathepsins: multifunctional enzymes in cancer. *Nat. Rev. Cancer* **6**, 764–775.
- Nakagawa, T., Roth, W., Wong, P., Nelson, A., Farr, A., Deussing, J., Villadangos, J.A., Ploegh, H., Peters, C., and Rudensky, A.Y. (1998). Cathepsin L: critical role in $\text{I}\alpha$ degradation and CD4 T cell selection in the thymus. *Science* **280**, 450–453.
- Petermann, I., Mayer, C., Stypmann, J., Biniössek, M.L., Tobin, D.J., Engelen, M.A., Dandekar, T., Grune, T., Schild, L., Peters, C., and Reinheckel, T. (2006). Lysosomal, cytoskeletal, and metabolic alterations in cardiomyopathy of cathepsin L knockout mice. *FASEB J.* **20**, 1266–1268.
- Reinheckel, T., Hagemann, S., Dollwet-Mack, S., Martinez, E., Lohmüller, T., Zlatkovic, G., Tobin, D.J., Maas-Szabowski, N., and Peters, C. (2005). The lysosomal cysteine protease cathepsin L regulates keratinocyte proliferation by control of growth factor recycling. *J. Cell Sci.* **118**, 3387–3395.
- Sadaghiani, A.M., Verhelst, S.H., Gocheva, V., Hill, K., Majerova, E., Stinson, S., Joyce, J.A., and Bogyo, M. (2007). Design, synthesis, and evaluation of *in vivo* potency and selectivity of epoxysuccinyl-based inhibitors of papain-family cysteine proteases. *Chem. Biol.* **14**, 499–511.
- Sevenich, L., Pennacchio, L.A., Peters, C., and Reinheckel, T. (2006). Human cathepsin L rescues the neurodegeneration and lethality in cathepsin B/L double-deficient mice. *Biol. Chem.* **387**, 885–891.
- Spira, D., Stypmann, J., Tobin, D.J., Petermann, I., Mayer, C., Hagemann, S., Vasiljeva, O., Gunther, T., Schule, R., Peters, C., and Reinheckel, T. (2007). Cell type-specific functions of the lysosomal protease cathepsin L in the heart. *J. Biol. Chem.* **282**, 37045–37052.
- Urbich, C., Heeschen, C., Aicher, A., Sasaki, K., Bruhl, T., Farhadi, M.R., Vajkoczy, P., Hofmann, W.K., Peters, C., Pennacchio, L.A., et al. (2005). Cathepsin L is required for endothelial progenitor cell-induced neovascularization. *Nat. Med.* **11**, 206–213.
- Vasiljeva, O. and Turk, B. (2008). Dual contrasting roles of cysteine cathepsins in cancer progression: apoptosis versus tumour invasion. *Biochimie* **90**, 380–386.
- Vasiljeva, O., Papazoglou, A., Kruger, A., Brodoefel, H., Korovin, M., Deussing, J., Augustin, N., Nielsen, B.S., Almholt, K., Bogyo, M., et al. (2006). Tumor cell-derived and macrophage-derived cathepsin B promotes progression and lung metastasis of mammary cancer. *Cancer Res.* **66**, 5242–5250.
- Vasiljeva, O., Reinheckel, T., Peters, C., Turk, D., Turk, V., and Turk, B. (2007). Emerging roles of cysteine cathepsins in disease and their potential as drug targets. *Curr. Pharm. Des.* **13**, 385–401.

Received December 17, 2007; accepted March 27, 2008